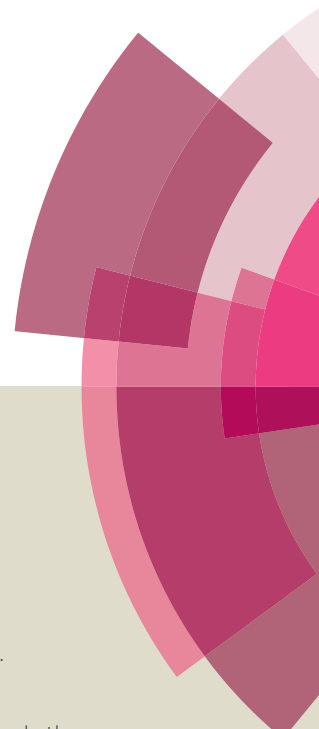
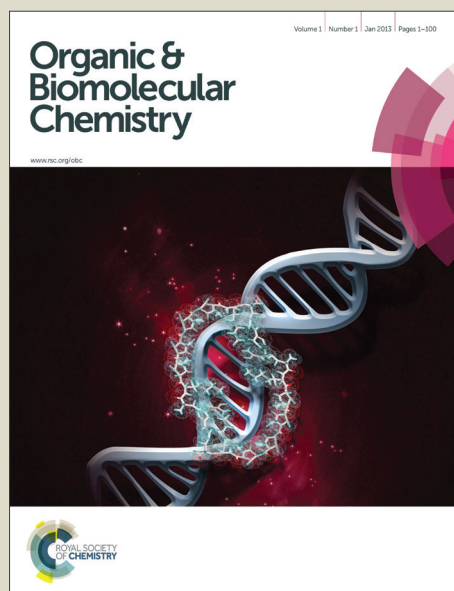


Organic & Biomolecular Chemistry

Accepted Manuscript



This article can be cited before page numbers have been issued, to do this please use: D. L. da Silva, B. S. Terra, M. R. Lage, A. L. Ruiz, C. C. da Silva, J. Carvalho, J. W. de M. Carneiro, F. T. Martins, S. A.



This is an *Accepted Manuscript*, which has been through the Royal Society of Chemistry peer review process and has been accepted for publication.

Accepted Manuscripts are published online shortly after acceptance, before technical editing, formatting and proof reading. Using this free service, authors can make their results available to the community, in citable form, before we publish the edited article. We will replace this *Accepted Manuscript* with the edited and formatted *Advance Article* as soon as it is available.

You can find more information about *Accepted Manuscripts* in the [Information for Authors](#).

Please note that technical editing may introduce minor changes to the text and/or graphics, which may alter content. The journal's standard [Terms & Conditions](#) and the [Ethical guidelines](#) still apply. In no event shall the Royal Society of Chemistry be held responsible for any errors or omissions in this *Accepted Manuscript* or any consequences arising from the use of any information it contains.

Cite this: DOI: 10.1039/c0xx00000x

www.rsc.org/xxxxxx

FULL PAPER

Xanthenones: Calixarenes-catalyzed Syntheses, Anticancer Activity and QSAR Studies

Daniel Leite da Silva,^a Bruna Silva Terra,^a Mateus Ribeiro Lage,^b Ana Lúcia Tasca Góis Ruiz,^c Cameron Capeletti da Silva,^d João Ernesto de Carvalho,^c José Walkimar de Mesquita Carneiro,^b Felipe Terra Martins,^d Sergio Antonio Fernandes,^e and Ângelo de Fátima^{*a}

Received (in XXX, XXX) XthXXXXXXXXXX 20XX, Accepted Xth XXXXXXXXXXXX 20XX

DOI: 10.1039/b000000x

An efficient method is proposed for obtaining tetrahydrobenzo[*a*]xanthene-11-ones and tetrahydro-[1,3]-dioxolo[4,5-*b*]xanthene-9-ones. The method is based on the use of *p*-sulfonic acid calix[*n*]arenes as catalysts under solvent-free condition. The antiproliferative activity of fifty-nine xanthenones against six human cancer cells was studied. The capacity of all compounds to inhibit cancer cells growth was dependent on the histological origin of cells. QSAR studies indicate that among compounds derived from β -naphthol the most efficient compounds against glioma (U251) and renal (NCI-H460) cancer cells are those having higher hydrogen bonding donor ability.

Introduction

Cancer is an important public health concern and a leading cause of death. It accounted for eight million deaths worldwide (*ca.* 15% of all deaths) in 2010 (38% more than in 1990).^{1,2} Many of current chemotherapy drugs have low specificity for tumor cancer cells, and are also toxic to normal cells. Related to the inefficiency of existing drugs against different types of cancer issues, as well as the increasing emergence of strains resistant to these drugs are also reported.³ Indeed, one of the biggest challenges of combating cancer is the development of new anticancer agents that are safe and effective.

Xanthenones are important biologically active heterocyclic compounds, with remarkable biological and medicinal properties, such as antiviral⁴, anti-inflammatory⁵, antiproliferative⁶ and antibacterial activities.⁷ Furthermore these compounds are also used as dyes⁸, as probes for fluorescence-based detection of biomolecules⁹ and in laser technologies.¹¹ Xanthenones are also investigated for agricultural purpose as bactericide agent⁷ and as photosensitizers in photodynamic therapy.¹¹

Multicomponent reaction (MCR) approaches, using a phenolic compound, aldehydes and 1,3-dicarbonyl compounds under acid-catalyst effect, are used for synthesis of xanthenes.¹²⁻¹⁴ In the recent years, use of calix[*n*]arenes as catalyst has received considerable interest in organic synthesis, particularly in MCRs.¹⁵ Calix[*n*]arenes are macrocyclic compounds synthesized by the *orto*-condensation of *para*-substituted phenols and formaldehyde under base conditions. There are a large number of applications involving calix[*n*]arenes due to their easy structural modification.¹⁵⁻¹⁷ In the last two decades, chemical literature has reported numerous applications of calix[*n*]arenes in supramolecular chemistry.¹⁸ Among all calix[*n*]arenes known so far, *p*-sulfonic acid calix[*n*]arenes showed to be the most efficient catalysts for Biginelli¹⁹, Povarov^{20,21}, Mannich-type²² and esterification²³ reactions. Although the use of calix[*n*]arenes as catalysts in various reactions, there is no report in the literature on the use of these compounds as catalysts in the synthesis of xanthenones.

^aGrupo de Estudos em Química Orgânica e Biológica (GEQOB), Departamento de Química, Instituto de Ciências Exatas, Universidade Federal de Minas Gerais, Belo Horizonte, MG, 31270-901, Brazil. Fax: +55-31-3409-5700; Tel: +55-31-3409-6373; E-mail: adefatima@qui.ufmg.br

^bInstituto de Química, Universidade Federal Fluminense, Campus do Valonguinho, Niterói, RJ, 24220-900, Brazil.

^cCentro Pluridisciplinar de Pesquisas Químicas, Biológicas e Agrícolas (CPQBA), Universidade Estadual de Campinas, Paulínia, SP, 13081-970, Brazil.

^dInstituto de Química, Universidade Federal de Goiás, Goiânia, GO, 74690-900, Brazil.

^eGrupo de Química Supramolecular e Biomimética (GQSB), Departamento de Química, Universidade Federal de Viçosa, Viçosa, MG, 36570-900, Brazil.

†CCDC reference numbers 945409-945410. See DOI: 10.1039/b000000x/

The facile synthesis based on MCR approaches and the diverse biological profile exhibited by xanthenones brought new perspectives for the development of new drugs based on this class of compounds. Herein, we report the synthesis of fifty-nine xanthenones and their *in vitro* antiproliferative activity was investigated on six human cancer cell types and some structure–activity relationship (SAR) studies were conducted.

Results and Discussion

We report herein an easy-to-do and solvent-free three-component synthesis of xanthenones in the presence of a catalytic quantity of the calix[*n*]arenes **CX1**–**CX6** (Figure 1). Xanthenones were synthesized using aldehydes, 1,3-dicarbonyl compound, β -naphthol or sesamol as a starting material. First we focused on the screening of a series of calix[*n*]arenes (Figure 1) as catalysts in reactions containing β -naphthol, 4-fluoro-benzaldehyde and dimedone at 120 °C under solvent-free conditions (Table 1). Among the calix[*n*]arenes tested in the range of 0.15–2.0 mol%, **CX3** and **CX6** were the most efficient catalysts. Both **CX3** and **CX6** at 1.5 mol% furnished the xanthenone **4** in 74% and 68% yields, respectively (Table 1; entries 5 and 10, respectively).

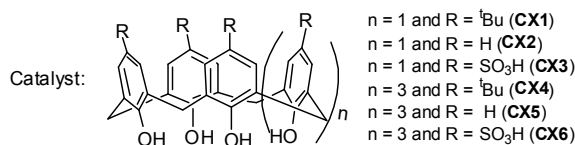


Figure 1. Structure of calix[*n*]arenes evaluated as catalyst.

Amounts of **CX3** or **CX6** lower than 1.0 mol% (Table 1; entries 2 and 3 for **CX3**, and entries 7 and 8 for **CX6**) or higher than 1.5 mol% (Table 1; entries 6 and 11, for **CX3** and **CX6**, respectively) provided **4** in poor to moderate yields. The yield of reactions in the presence of 1.5 mol% calix[*n*]arenes **CX1**, **CX2**, **CX4** or **CX5** was comparable to that of catalyst-free reactions (Table 1; entry 1).

We also evaluated whether calix[*n*]arenes **CX3** or **CX6** could be reused in such reactions. After completing the reaction, CHCl_3 and water were added to the mixture for recovering **CX3** or **CX6** in the aqueous phase from the reaction medium. Once dried, the residue was used in successive reactions in which the yields were monitored. **CX3** and **CX6** were successfully used in three successive reactions without significant loss of catalyst activity (Figure 2).

Table 1. Effect of the quantity of *p*-sulfonic acid calix[*n*]arenes of xanthenone **4** based on the amount of catalyst.

Entry	Catalyst (mol%)	Yield ^a (%)
1	--	16
2	CX3 (0.15)	53
3	CX3 (0.5)	57
4	CX3 (1.0)	61
5	CX3 (1.5)	74
6	CX3 (2.0)	63
7	CX6 (0.15)	54
8	CX6 (0.5)	61
9	CX6 (1.0)	64
10	CX6 (1.5)	68
11	CX6 (2.0)	67

Reagents and conditions: β -naphthol/4-fluoro-benzaldehyde/dimedone (molar ratio of 1.2:1.0:1.5), 120 °C for 1 h. ^aIsolated yield.

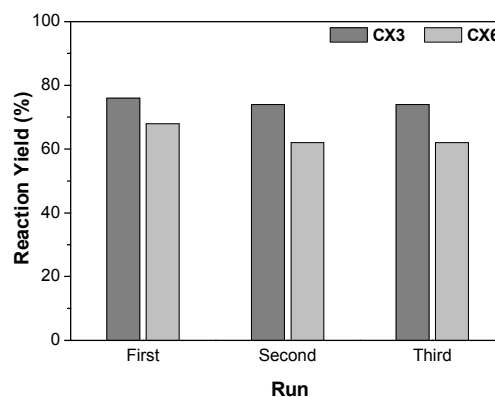


Figure 2. Reuse of *p*-sulfonic acid calix[*n*]arenes **CX3** and **CX6** in the synthesis of xanthenone **4**.

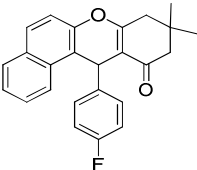
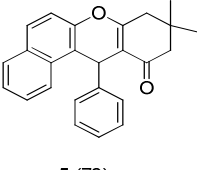
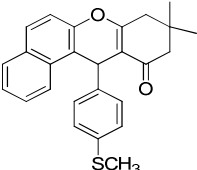
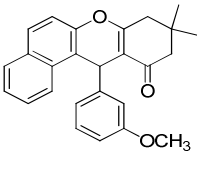
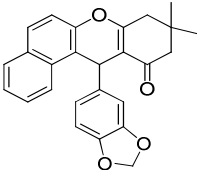
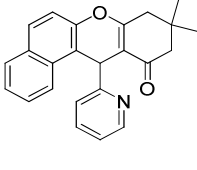
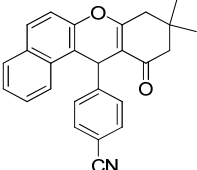
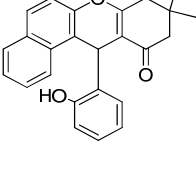
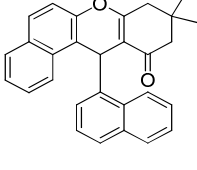
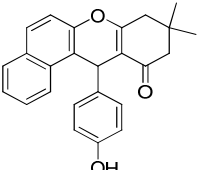
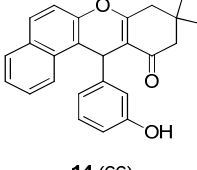
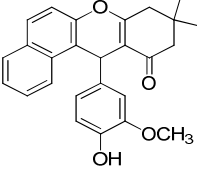
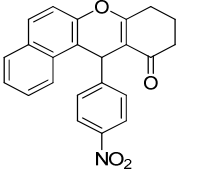
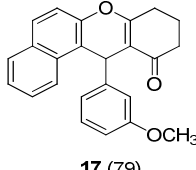
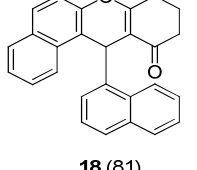
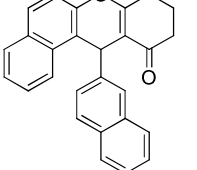
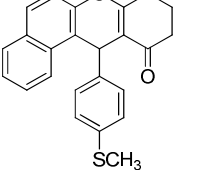
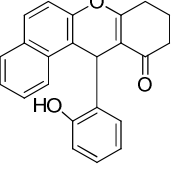
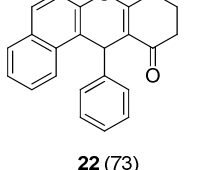
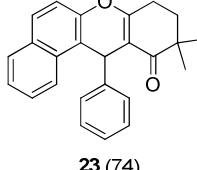
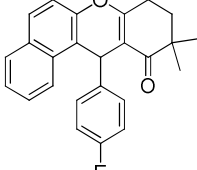
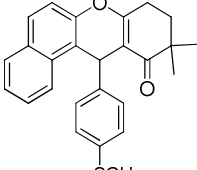
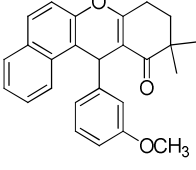
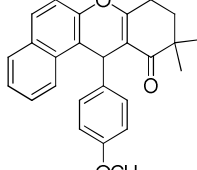
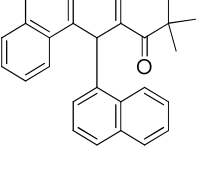
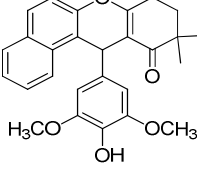
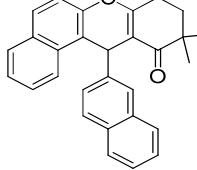
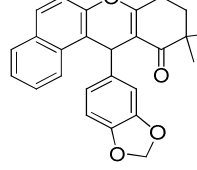
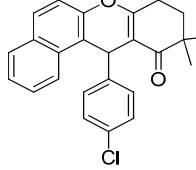
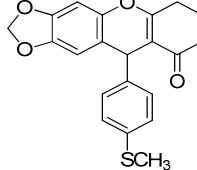
Considering that yields of reactions in the presence of either **CX3** or **CX6** were roughly the same (Table 1, entries 5 and 10, respectively) we chose the former to evaluate the scope of *p*-sulfonic acid calix[4]arene for the synthesis of xanthenones. Thus, a variety of aldehydes, 1,3-dicarbonyls and two phenolic compounds were used (Table 2). Fifty-nine xanthenones (**4**–**62**) were synthesized with yields in the range of 58 to 92%. The reaction yields were not considerably affected by the presence of electron-withdrawing or electron-donating groups in the aldehydes (Table 2).

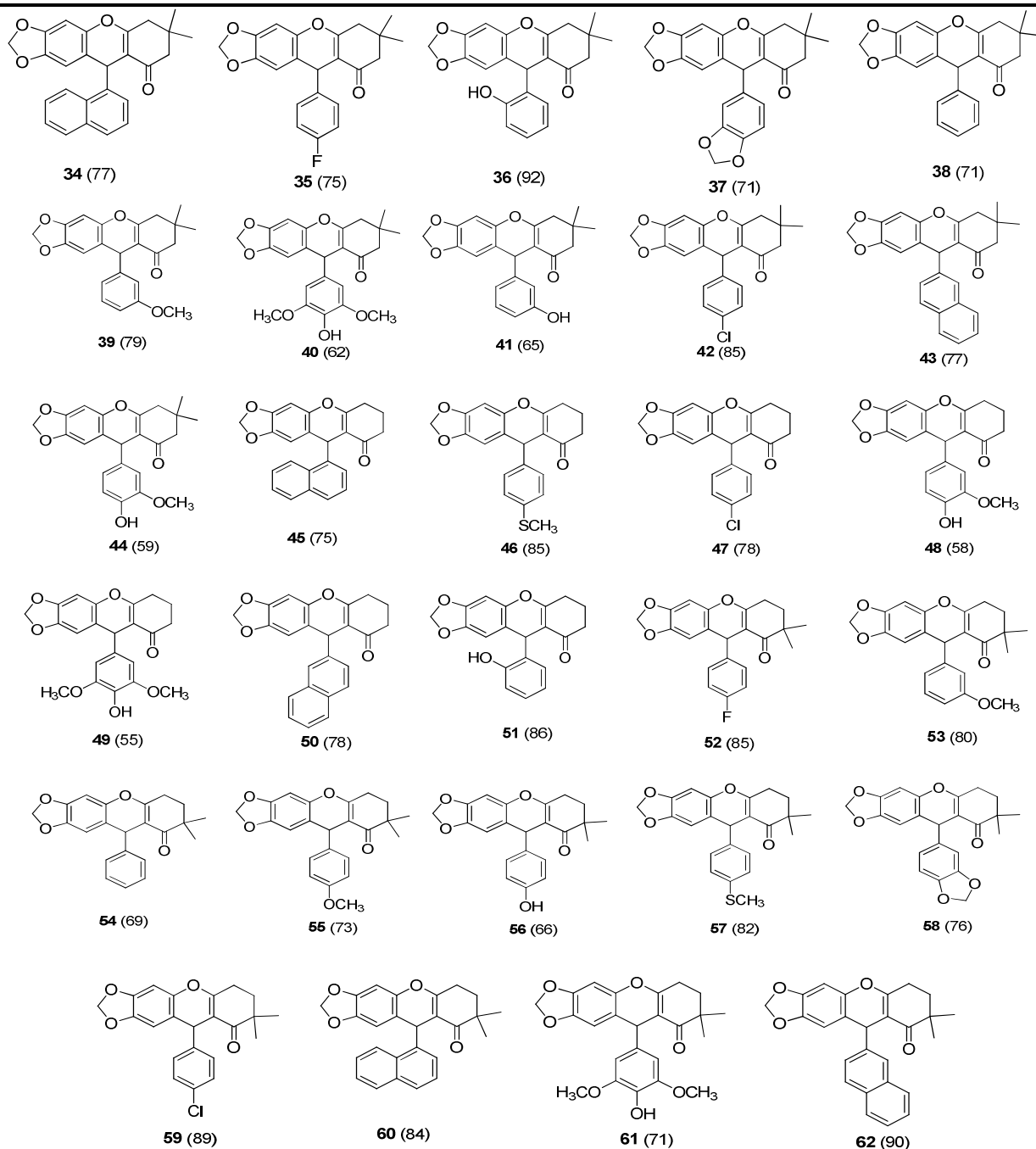
Cite this: DOI: 10.1039/c0xx00000x

www.rsc.org/xxxxxx

ARTICLE TYPE

Table 2. Synthesis of xanthenones catalyzed by the *p*-sulfonic acid calix[4]arene CX3.

 4 (74)	 5 (73)	 6 (68)	 7 (64)	 8 (71)
 9 (67)	 10 (76)	 11 (86)	 12 (80)	 13 (71)
 14 (66)	 15 (58)	 16 (70)	 17 (79)	 18 (81)
 19 (84)	 20 (73)	 21 (83)	 22 (73)	 23 (74)
 24 (78)	 25 (90)	 26 (82)	 27 (84)	 28 (88)
 29 (59)	 30 (82)	 31 (79)	 32 (81)	 33 (81)



Reagents and conditions: phenolic compound/aldehyde/1,3-dicarbonyl compound (molar ratio of 1.2:1.0:1.5), 120 °C for 1 h. The yield for obtaining each xanthenone is presented in parentheses.

Once synthesized, the structural characterizations of the xanthenones were determined from the corresponding IR, NMR (^1H and ^{13}C) and ESI-HRMS data. Crystals of **4** were also obtained and its crystal structure was determined using single-crystal X-ray diffractometry. Crystal data and refinement results are provided as supporting information (Table S1). Xanthenone **4** crystallizes in the triclinic system (space group P1). Both *R* and *S* enantiomers are present in the chosen crystallographic asymmetric unit (Figure 3). Their molecular conformation is similar. Moreover, they can not be related by centrosymmetry in

the crystal lattice. Therefore, crystal structure could not be solved in the centrosymmetric triclinic space group with only one molecule in the asymmetric unit. The xanthenone core, formed with the four fused rings labeled as A-D in Figure 3, is approximately planar, except for ring A which assumes a half-chair conformation with C3 deviating away from the least-squares plane calculated through the other five coplanar atoms of this ring by -0.631(7) Å in the *R*-enantiomer (atom labels ending with suffix A) and 0.660(6) Å in the *S*-enantiomer (atom labels ending with suffix B) (r.m.s.d. of the C2-C1-C6-C5-C4 fitted

Cite this: DOI: 10.1039/c0xx00000x

www.rsc.org/xxxxxx

ARTICLE TYPE

atoms is 0.0292 Å in the *R*-enantiomer and 0.0205 Å in the *S*-enantiomer). Ring B is not completely planar in both enantiomers, with C7 carbon deviating by -0.270(6) Å in the *R*-enantiomer and 0.212(6) Å in the *S*-enantiomer from the least-square mean plane calculated through the C6-C5-O2-C9-C8 atoms (r.m.s.d. of the fitted atoms is 0.0431 Å in the *R*-enantiomer and 0.0270 Å in the *S*-enantiomer). Taking the xanthenone mean plane is taken as reference, the out-of-plane C3 and C7 carbons are on the same side of the fluorinated phenyl ring in both enantiomers. Another intramolecular feature common to both enantiomers is the substituted phenyl ring conformation. Ring E is almost perpendicular to the xanthenone mean plane, forming an angle of 82.04(12)° in the *R*-enantiomer and 84.33(17)° in the *S*-enantiomer with the least-square plane calculated through the planar non-hydrogen atoms of the four fused rings A-D. Therefore, C3 and C7 were not included in this mean plane calculation.

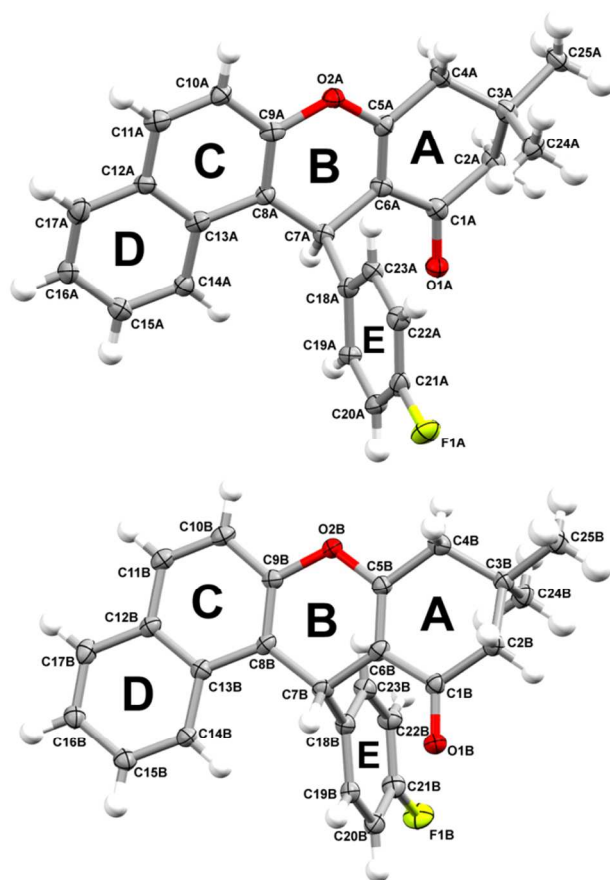


Figure 3. The two crystallographically independent molecules of compound 4. Ellipsoids of 30% probability and arbitrary radius spheres represent non-hydrogen and hydrogen atoms, respectively. Rings are also arbitrarily labeled.

Antiproliferative activity

Although xanthenones are known as bioactive heterocyclic compounds, only few works explored the potential of this class of compounds against cancer cells. Based on this, the antiproliferative effect of a series of synthesized xanthenones were investigated on glioma (U251), breast (MCF-7), multiple drugs-resistant ovarian (NCI-ADR/RES), renal (786-0), lung non-small cells (NCI-H460), colon (HT-29), and keratinocyte (HaCaT). Cell proliferation was determined by the sulforhodamine B method and doxorubicin (Dox) used as a positive control.²⁴

Initially the fifty-nine xanthenones synthesized were subdivided into two groups of compounds according to the precursor phenol structure. Group 1 was constituted of β -naphthol-derived xanthenones (4-32; Table 2) while 33-62 (Table 2), sesamol derivatives, were included in Group 2. The concentration of the most active xanthenones that elicited 50% cell growth inhibition (GI₅₀) is summarized in Table 3. The GI₅₀ values for the remainder compounds tested are provided as supporting information (Table S2).

When analyzing the data obtained for compounds of Group 1 (Table 3) noted that the NCI-ADR/RES cell line was the most sensitive cancer cells as attested by the number of compounds that negatively affected cells growth at GI₅₀ ≤ 10 µg/mL (Table 3). NCI-H460 cells were the least sensitive to compounds of Group 1 (Table 3).

For NCI-ADR/RES nineteen compounds of Group 1 showed GI₅₀ values lower than 10 µg/mL. The active compounds of Group 1 for this strain showed GI₅₀ values in the range of 0.027 to 9.8 µg/mL. Among the active compounds of Group 1 for NCI-ADR/RES cell line compound 5 was the most potent, with an GI₅₀ value of 0.027 µg/mL, its GI₅₀ value was found to be in the same order of magnitude of that for doxorubicin (GI₅₀ = 0.047 µg/mL) (Table 3). Indeed, xanthenone 5 showed high selectivity index for NCI-ADR/RES cancer cells, presenting weak antiproliferative activity against non-tumorigenic HaCat cells (Table 3). Xanthenones 7, 9, 13, 15, 16, 23 and 29 were also promising against NCI-ADR/RES cells by exhibiting GI₅₀ around 1 µg/mL (Table 3). Xanthenones 13, 15, and 29 were the most potent compounds against NCI-H460 cells; its GI₅₀ value were lower than 5.0 µg/mL. MCF7 cells were highly sensitive to xanthenones 8, 9, 13-15, 24 and 29 (Table 3). Compounds 13-15, 20 and 29 compromised U251 cells growth by 50% when used at concentrations lower than 6.5 µg/mL, while 786-0 cells were sensitive to 4, 6, 8, and 29. For HT-29 cells compounds 13-15, and 29 were the most potent with GI₅₀ values lower than 4.0 µg/mL. Among the tested compounds of Group 1, xanthenones 13, 15, 29 were those that exhibited the largest

spectrum of action. These xanthenones showed considerable antiproliferative activity ($GI_{50} < 10 \mu\text{g/mL}$) against all the cancer cell lines, except for kidney cancer cell line (786-0) in which xanthenones **13** and **15** presented GI_{50} values of 216.0 and 29.8 $\mu\text{g/mL}$, respectively (Table 3).

The second group of xanthenones evaluated (Group 2) is related with those compounds derived from sesamol (Table 3, compounds **33-62**). The antiproliferative activity of these compounds was expressed as the concentration that produced 50% cell growth inhibition or a cytostatic effect (GI_{50} , $\mu\text{g/mL}$) for each cell line (Table 3). Data obtained for compounds of Group 2 (Table 3) shows that MCF7 was the most sensitive cancer cells as attested by the number of compounds that negatively affected cells growth at $GI_{50} \leq 10 \mu\text{g/mL}$. Nine compounds were active against MCF7, and **48** was the most potent with GI_{50} of 0.7 $\mu\text{g/mL}$. Compounds **48** also compromised U251, NCI-ADR/RES, and HT-29 cells growth by 50% when used at concentrations lower than 1.0 $\mu\text{g/mL}$ while NCI-ADR/RES cells were sensitive to other six compounds **36**, **39**, **41**, **43** e **45**, and **49**. For HT-29 cells compounds **41**, **45**, **49** and **56** were the most potent with GI_{50} values lower than 4.0 $\mu\text{g/mL}$. Kidney cells (786-0) was the less sensitive strain to compounds of Group 2, for this line only compounds **41**, **48** and **49** were active, with GI_{50} values of 4.0, 2.2 and 7.1 $\mu\text{g/mL}$, respectively. For NCI-H460 strain compounds **41**, **48**, **49** and **56** were active compounds of Group 2. Compounds **48** ($GI_{50} = 2.3 \mu\text{g/mL}$) and **56** ($GI_{50} = 3.1 \mu\text{g/mL}$) exhibited GI_{50} values lower than 4.0 $\mu\text{g/mL}$, thus showing potent anticancer activity. Among compounds of Group 2, **41**, **48** and **49** were that showing the highest spectrum of action, which were active against the six cancer cell lines evaluated. Compound **48** showed GI_{50} values lower than 4.0 $\mu\text{g/mL}$ for all tested strains and can therefore be described as the most promising compound among compounds of Group 2.

The selectivity index (SI) was calculated for each compound of Group 1 and 2 (Table 3). Among evaluated xanthenones, compound **5** showed the highest SI value for NCI-ADR/RES cells, which indicated the potential use of this compound for future *in vivo* tests.

When compared the results obtained for compounds of Group 1 and 2, we can see that in general compounds of Group 1 were more active than the compounds of Group 2. Among compounds of Group 1 evaluated eight compounds showed no activity against any of the tested strains, where eighteen compounds of Group 2 were inactive for all cell lines evaluated. Together these results suggest that the naphthyl nucleus is important for the antiproliferative activity of this class of compound. Overall, the potency of xanthenones was dependent on the histological origin of cancer cells.

QSAR Studies.

For a more careful analysis of the relationship between molecular structure and biological activity, QSAR studies were performed. To determine the correlation between molecular descriptors and the efficiency of the set of xanthenones, we tested a set of models as discussed below.

At first, a structural analysis of the studied compounds was carried out. The geometries of the 59 synthesized compounds were obtained from AM1 semiempirical calculations, after a conformational analysis using the conformer distribution subroutine of the SPARTAN'06 software. The most stable conformation of each derivative was then reoptimized with the MOPAC software, again using the AM1 method. The outputs files from the MOPAC calculation were used to generate a set of molecular descriptors by using the CODESSA software.

CODESSA may generate about 400 molecular descriptors associated with molecular constitution, geometry, and topology and with electrostatic, thermodynamic, and quantum chemical parameters. The molecular descriptors generated by CODESSA were correlated to the biological efficiency using the heuristic method.²⁵ Models based on a single molecular descriptor were chosen to obtain statistically significant meanings. After elimination of descriptors with low variance or high intercorrelation, the best correlations were found with the molecular descriptors for compounds of Group 1 to cell lines U251 and NCI-H460. Compounds with $GI_{50} > 250 \mu\text{g/mL}$ were not considered in QSAR studies.

For U251 the best correlation was between experimental biological activity of compounds of Group 1 and the calculated efficiency based on the molecular descriptor HDCA-1.

HDCA-1 is a molecular descriptor that reports the hydrogen bonding donor ability of the molecule. The values of this descriptor are obtained as a sum of the accessible surface area of H-bonding donor H atoms, as described below.^{26,27}

$$HDCA1 = \sum_D s_D \quad D \in H_{H-donor}$$

where

s_D – solvent-accessible surface area of H-bonding donor H atoms.

The model obtained for U251 cells is given in Figure 4 with the corresponding calculated *versus* measured efficiency plots.

This correlation indicates that the increasing the accessible surface area of hydrogen bond donor atoms ($HDCA1$) leads to an increase in biological activity of the compound. This model shown to be consistent with the fact that compounds **13**, **14**, **15**, and **29** which have a hydroxyl group in the *meta* or *para* position and have the highest values of HDCA1 molecular descriptor were the most active against U251 cells. Although compounds **11** and **21** possess a hydroxyl group in the *ortho* position, this is less accessible than the *meta* or *para* positions resulting in lower values for the descriptor HDCA1 and experimental biological activity.

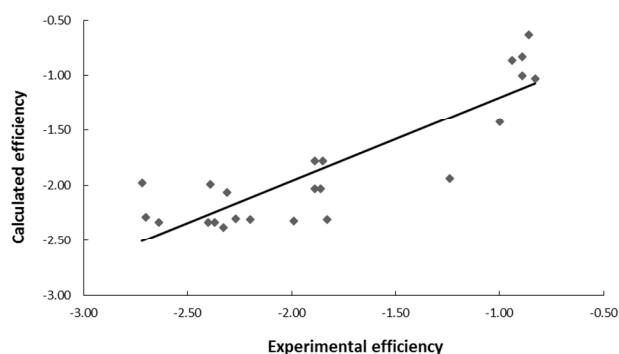
Table 3. Selective index (SI)^a and concentration of the most active xanthenones (GI₅₀^b in µg/mL) that elicits cancer cells^c growth inhibition by 50%.

Group	Xanthene	U251		MCF7		NCI-ADR/RES		786-0		NCI-H460		HT-29		HaCaT
		GI ₅₀	SI	GI ₅₀	SI	GI ₅₀	SI	GI ₅₀	SI	GI ₅₀	SI	GI ₅₀	SI	
1	4	186.6	0.2	203.7	0.2	2.0	16.1	3.1	10.3	36.3	0.9	>250	<0.1	32.1
1	5	56.8	0.8	92.0	0.5	0.03	1626	28.9	1.5	85.8	0.5	>250	<0.2	43.9
1	6	>250	<0.4	61.4	1.6	>250	<0.4	2.8	35.3	81.7	1.2	>250	0.4	98.9
1	7	29.8	1.8	56.9	1.0	0.8	70.3	>250	<0.2	50.5	1.1	>250	<0.2	54.1
1	8	28.5	0.9	2.0	12.9	227.9	0.1	1.7	15.1	28.7	0.9	48.2	0.5	25.7
1	9	25.6	0.9	5.2	4.5	0.7	33.3	27.1	0.9	31.4	0.7	29.9	0.8	23.3
1	11	14.0	3.8	>250	<0.2	67.5	0.8	225.4	0.2	>250	<0.2	>250	<0.2	52.9
1	13	2.9	2.1	2.6	2.3	0.4	15.2	216.0	0.03	2.8	2.2	3.2	1.9	6.1
1	14	2.9	2.0	2.7	2.1	6.7	0.9	>250	<0.02	13.1	0.4	3.2	1.8	5.8
1	15	2.9	6.9	3.9	5.2	0.3	67.0	29.8	0.7	2.6	7.7	3.4	5.9	20.1
1	16	94.0	2.7	100.3	2.5	0.4	625	197.4	1.3	119.9	2.1	>250	-	>250
1	20	6.5	4.4	21.5	1.3	8.9	3.2	20.4	1.4	19.6	1.4	16.0	1.8	28.4
1	21	84.5	2.4	127.0	1.6	51.9	3.9	246.3	0.8	>250	<0.8	>250	<0.8	204.6
1	23	35.1	1.0	82.4	0.4	0.1	341	188.3	0.2	60.3	0.6	95.9	0.4	34.1
1	24	25.1	0.6	8.8	1.8	4.4	3.5	76.6	0.2	44.2	0.3	16.2	1.0	15.4
1	29	2.9	2.4	2.8	2.5	0.4	17.8	4.9	1.4	4.3	1.7	2.9	2.4	7.1
2	36	25.2	1.1	24.4	1.1	9.3	2.9	26.2	1.0	24.3	1.1	19.4	1.4	26.6
2	39	37.2	0.3	5.7	2.3	7.2	1.8	110.3	0.1	27.8	0.5	4.9	2.6	12.9
2	41	3.4	1.2	3.0	1.3	4.9	0.8	4.0	1.0	5.0	0.8	3.5	1.1	4.0
2	43	29.5	1.1	26.3	1.2	8.6	3.8	28.5	1.1	26.1	1.2	25.1	1.3	32.6
2	45	5.3	0.8	3.2	1.3	5.4	0.8	25.0	0.1	10.5	0.4	2.6	1.7	4.3
2	48	0.7	1.1	0.7	1.1	0.5	1.6	2.2	0.4	2.3	0.3	0.43	1.9	0.80
2	49	3.3	0.8	2.2	1.3	1.6	1.8	7.1	0.4	7.3	0.4	2.7	1.0	2.8
2	56	3.3	1.1	2.9	1.2	12.9	0.3	>250	<0.01	3.1	1.1	2.7	1.3	3.5
-	Dox ^d	0.03	7.4	0.06	3.4	0.05	4.0	0.04	5.3	0.01	15.4	0.08	2.4	0.2

^aSelectivity index was determined as the ratio of the GI₅₀ for HaCat to the GI₅₀ for the cancer cell line. ^bGI₅₀ values were obtained from two independent experiments, each done in triplicate. ^cU251, glioma cells; MCF7, breast; NCI-ADR/RES, multiple drug-resistant ovarian cancer cells; 786-0, renal cancer cells; NCI-H460, non-small lung cancer cells; HT-29, colon cancer cells; HaCaT, keratinocyte. ^dReference drug.

$$\log\left(\frac{1}{IC_{50}}\right) = 6.49e - 1(\pm 8.41e - 02)(HDCA1) - 2.46e + 00(\pm 1.01e - 01)$$

$$n = 23; r^2 = 0.764; F = 68.1; s^2 = 0.1067; R^2_{CV} = 0.731$$

**Figure 4.** Experimental versus calculated efficiency with the HDCA1 descriptor.

The best correlation found for NCI-H460 cells was between the experimental biological activity of compounds of Group 1 and the calculated efficiency based on the molecular descriptor HDCA2. HDCA2 is a molecular descriptor based on accessible area of hydrogen-bond donor atoms and corresponds to partial

charges.^{26,27} HDCA2 descriptor can be calculated as described

$$\text{below. } HDCA2 = \sum_D \frac{q_D \sqrt{S_D}}{\sqrt{S_{tot}}} \quad D \in H_{H-donor}$$

where

S_D - solvent-accessible surface area of H-bonding donor H atoms

q_D - partial charge on H-bonding donor H atoms

S_{tot} - total solvent-accessible molecular surface area

The model obtained for NCI-H460 cells is given in Figure 5. This relation indicates that the activity values increase when increasing the value of the molecular descriptor HDCA2. This behavior is similar to that shown for U251 cells and the HDCA1 molecular descriptor. Again compounds **13**, **14**, **15**, and **29** which have a hydroxyl group in the *meta* or *para* positions and have the highest values of HDCA2 molecular descriptor were the most active against NCI-H460 cells and *ortho* hydroxylated compounds **11** and **21** were less active than *meta* or *para* hydroxylated derivatives. In summary these two models shows that the activity of compounds of Group 1 against U251 and NCI-H460 increased with the increasing in accessible surface area of hydrogen bond donor atoms.

$$\text{Log} \left(\frac{1}{IC_{50}} \right) = 4.00e + 00(\pm 5.06e - 01)(\text{HDCA2}) - 2.74e + 00(\pm 1.39e - 01)$$

$$n = 22; r^2 = 0.758; F = 62.5; s^2 = 0.159; R^2_{cv} = 0.639$$

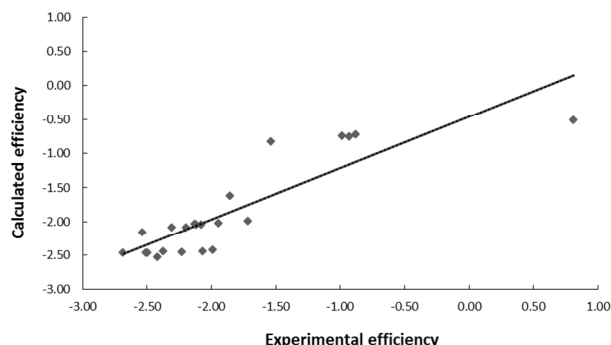


Figure 5. Experimental *versus* calculated efficiency with the HDCA2 descriptor.

Conclusions

An efficient method was described for the synthesis of fifty nine xanthenones under mild conditions. The reaction yields dramatically increased upon the use of *p*-sulfonic acid calix[*n*]arenes as catalysts. Some advantages of the approach here described include absence of solvents and metal catalysts, short reaction time, catalyst tolerance of a wide range of functional groups and catalyst recycling as well. The ability to inhibit the growth of cancer cells were also investigated for synthesized compounds. Compound **5** was as potent as the reference drug doxorubicin against NCI-ADR/RES and present the greater value of SI. Several compounds were shown to be active against different cancer cell lines indicating that the capacity to inhibit cancer cells growth of the xanthenones was dependent on the histological origin of cells. In general xanthenones derivatives of β -naphthol were more active than derived from sesamol. A QSAR study was performed and two QSAR models were obtained for compounds of Group 1 against U251 and NCI-H460 cells and indicated that the biological activity of compounds increased with increasing accessible surface area of hydrogen bond donor atoms. These results show some xanthenones as lead compounds for obtaining new anticancer agents.

Experimental

General methods and materials

All starting materials were obtained from commercially available sources with high-grade purity and used without further purification. Calix[*n*]arenes **CX1-CX6** were prepared according to known procedures.^{28,29,30} Reactions did not require anhydrous conditions. The melting points (uncorrected) of synthesized xanthenones were determined on a Mettler FP 80 HT apparatus. Infrared spectra were recorded on a Perkin Elmer Spectrum One spectrophotometer (KBr). The ¹H and ¹³C-NMR spectra were recorded on a Bruker AVANCE DPX-200 spectrometry at 200 MHz to ¹H and 50 MHz to ¹³C, in DMSO-*d*₆, CDCl₃ or pyridine-

*d*₅. Coupling constants (*J*) are reported in Hertz (Hz). High resolution mass spectra (HRMS) were recorded on Shimadzu LC-IT-TOF Prominence system. Low temperature X-ray diffraction data were collected using an Enraf-Nonius Kappa-CCD diffractometer equipped with a CCD camera of 95 mm and κ -goniostat. No absorption correction was applied to the raw dataset due to the negligible absorption coefficient using graphite-monochromated Mo K α beam (λ =0.71073 Å). The structure was solved using the direct methods of phase retrieval and the model was refined by full-matrix least squares method based on F². Positions of hydrogens have followed a riding model with bond distances stereochemically constrained according to the bonded carbon. The isotropic thermal displacement parameters of hydrogens were either 20% (C-H hydrogens, except those in methyl moieties) or 50% (hydrogens in methyl moieties) greater than the equivalent isotropic parameter of the bonded carbon.

General procedure for the synthesis of xanthenones

A mixture of an aromatic aldehyde (1 mmol), 1,3-dicarbonyl compound (1.5 mmol) and β -naphthol or sesamol (1.2 mmol) and *p*-sulfonic acid calix[*n*]arene **CX3** or **CX6** (1.5 mol%) was stirred at 120 °C for 1 h. After completion of the reaction, methanol and was added to the mixture and stirred for 30 min. Then the solid was filtered and washed with cold ethanol to afford the xanthenones **4-62** in high purity (Table 3). All xanthenones were characterized by ¹H, ¹³C NMR, IR, HRMS (ESI) and melting point (see Supporting Information for reference).

Antiproliferative assay

Human tumor cell lines U251 (glioma), MCF-7 (breast) NCI-ADR/RES (multiple drugs-resistant ovarian), 786-0 (renal), NCI-H460 (lung, non-small cells), HT-29 (colon), and HaCaT (keratinocyte) were kindly provided by Frederick Cancer Research & Development Center-National Cancer Institute-Frederick, MA, USA. Stock cultures were grown in RPMI 1640 (GIBCO BRL, Life Technologies) supplemented with 5% of fetal bovine serum and penicillin (final concentration of 1 mg/mL) and streptomycin (final concentration of 200 U/mL).^{31,32} Cells in 96-well plates (100 μ L cells/well) were exposed to Biginelli adducts (0.25–250 μ g/mL) for 48 h at 37 °C and 5% of CO₂. Afterward cells were fixed with 50% trichloroacetic acid, submitted to sulforhodamine B assay for cell proliferation quantitation at 540 nm.²⁴ The concentration of compound that inhibits cell growth by 50% (GI₅₀) was determined through non-linear regression analysis using software ORIGIN 7.5 (OriginLab Corporation). Doxorubicin was used as a reference drug. Results presented are from two independent experiments, each done in triplicate.

Computations.

The conformational analysis of the 59 xanthenones was done using the conformer distribution subroutine of the SPARTAN'06 software.³³ The most stable conformation of each derivative was selected for further calculations with the MOPAC code³⁴, again using the AM1³⁵ semiempirical method. In this new step the geometry optimization was developed with the MOPAC code and

Cite this: DOI: 10.1039/c0xx00000x

www.rsc.org/xxxxxx

ARTICLE TYPE

all structures were confirmed as a local minimum by calculation of the Hessian matrix force constant (no negative eigenvector).³⁶ Two sets of output files were obtained with the MOPAC code. In the first one the following keywords were used: AM1, PRECISE, XYZ, EF, ENPART, VECTORS, BONDS, PI, and POLAR. In the second one, which was used to calculate the thermodynamic properties, the following keywords were used: AM1, PRECISE, THERMO, ROT=1, and XYZ. These output files from MOPAC calculations were used to the development of the initial CODESSA calculations, to generate a set of molecular descriptors used in the QSAR analysis, also developed by using the CODESSA software.³⁷ In the statistical analysis for the QSAR study the following parameters were employed: maximum number of descriptors per model, 1; criterion of significance of parameter, 0.01; level of high correlation, 0.99; level of intercorrelation significance, 0.8.

Acknowledgements

We acknowledge the following Brazilian agencies: Conselho Nacional de Desenvolvimento Científico e Tecnológico (CNPq) for research fellowships (A.D.F., J.W.M.C., S.A.F.) and financial support; Fundação de Amparo à Pesquisa de Minas Gerais (FAPEMIG), Coordenação de Aperfeiçoamento de Pessoal de Nível Superior (Capes), and Fundação de Amparo à Pesquisa do Estado do Rio de Janeiro (FAPERJ). Authors are also thankful to Dr. C.M. da Silva and L.S. Neto for critical reading of the manuscript.

References

1. R. Lozano, M. Naghavi, K. Foreman, *et al.*, *Lancet*, 2013, **380**, 2095-2128.
2. O. Nakash, I. Levav, S. Aguilar-Gaxiola, *et al.*, *Psychooncology*, 2014, **23**, 40-51.
3. B. A. Chabner, J. T. G. Roberts, *Nat. Rev. Cancer.*, 2005, **5**, 65-72.
4. R. W. Lambert, J. A. Martin, J. H. Merrett, K. E. B. Parkes, G. J. Thomas, *CT Int. Appl. WO9706178*, 1997.
5. J. P. Poupelin, G. Saint-Rut, O. Fussard-Blanpin, G. Narcisse, Uchida-Ernouf, G. R. Lakroix, *Eur. J. Med. Chem.*, 1978, **13**, 67-71.
6. A. Kumar, S. Sharma, R. A. Maurya, J. Sarkar, *J. Comb. Chem.*, 2010, **12**, 20-24.
7. T. Hideo, J. Teruomi, *Jpn. Patent 56.005.480*, 1981.
8. A. Banerjee, A. K. Mukherjee, *Biotechnic & Histochemistry* 1981, **56**, 83-85.
9. C. G. Knight, T. Stephens, *Biochem. J.* 1989, **258**, 683-689.
10. O. Sirkencioglu, N. Talinli, A. J. Akar, *Chem. Res.* 1995, **12**, 502.
11. R. M. Ion, A. Planner, K. Wiktorowicz, D. Frackowiak, *Acta Biochim. Pol.* 1998, **45**, 833-845.
12. M. M. Heravi, H. Alinejhad, K. Bakhtiari, M. Saeedi, H. A. Oskooie, F. F. Bamoharram, *Bull. Chem. Soc. Ethiop.*, 2011, **25**, 399-406.
13. J. M. Khurana, D. P. Magoo, *Tetrahedron Lett.*, 2009, **50**, 4777-4780.
14. Z-H. Zhang, H-J. Wang, X-Q. Ren, Y-Y. Zhang, *Monatshefte für Chem.*, 2009, **140**, 1481-1483.
15. J. B. Simões, D. L. da Silva, A. de Fátima, S. A. Fernandes, *Curr. Org. Chem.* 2012, **16**, 949-971.
16. A. de Fátima, S. A. Fernandes, A. A. Sabino, *Curr. Drug. Discov. Tech.* 2009, **6**, 151-170.
17. E. V. V. Varejão, A. de Fátima, S. A. Fernandes. *Curr. Pharm. Des.* 2013, **19**, 6507-6521.
18. P. Jose, S. Menon, *Bioinorg. Chem. Appl.* 2007, **28**, 1-16.
19. D. L. da Silva, S. A. Fernandes, A. A. Sabino, A. de Fátima, *Tetrahedron Lett.* 2011, **52**, 6328-6330.
20. J. B. Simões, A. de Fátima, A. A. Sabino, F. J. T. Aquino, D. L. da Silva, L. C. A. Barbosa, S. A. Fernandes. *Org. Biomol. Chem.* 2013, **11**, 5069-5073.
21. J. B. Simões, A. de Fátima, A. A. Sabino, L. C. A. Barbosa, S. A. Fernandes. *RSC Adv.* 2014, **4**, 18612-18615.
22. S. Shimizu, N. Shimada, Y. Sasaki, *Green Chem.* 2006, **8**, 608-614.
23. S. A. Fernandes, R. Natalino, P. A. R. Gazolla, M. J. da Silva, G. N. Jham, *Tetrahedron Lett.* 2012, **53**, 1630-1633.
24. A. Monks, D. Scudeiro, P. Skehan, R. Shoemaker, K. Paull, D. Vistica, C. Hose, J. Langley, P. Cronise, A. Vaigro-Wolff, M. Gray-Goodrich, H. Campbelli, J. Mayo, M. J. Boyd, *J. Nat. Cancer Inst.* 1991, **83**, 757-766.
25. B. Xia, W. Ma, B. Zheng, X. Zhang, B. Fan, *Eur. J. Med. Chem.*, 2008, **43**, 1489-1498.
26. D. T. Stanton, P. C. Jurs, *Anal. Chem.*, 1990, **62**, 2323.
27. D. T. Stanton, L. M. Egolf, P. C. Jurs, M. G. Hicks, *J. Chem. Inf. Comput. Sci.*, 1992, **32**, 306.
28. C. D. Gutsche, B. Dhawan, K. H. No, R. Muthukrishnan, *J. Am. Chem. Soc.*, 1981, **103**, 3782-3792.
29. A. Casnati, N. D. Ca, F. Sansone, F. Ugozzoli, R. Ungaro, *Tetrahedron*, 2004, **60**, 7869-7876.
30. S. Shinkai, K. Araki, T. Tsubaki, T. Some, O. Manabe, *J. Chem. Soc. Perkin Trans 1*, 1987, 2297-2299.
31. D. L. da Silva, F. S. Reis, D. R. Muniz, A. L. T. G. Ruiz, J. E. de Carvalho, A. A. Sabino, L. V. Modolo, A. de Fátima, *Bioorg. Med. Chem.*, 2012, **20**, 2645-2650.
32. S. R. Pacheco, T. C. Braga, D. L. da Silva, L. P. Horta, F. S. Reis, A. L. T. G. Ruiz, J. E. de Carvalho, L. V. Modolo, A. de Fátima, *Med. Chem.*, 2013, **9**, 889-896.
33. *Spartan '06* Wavefunction, Inc. Irvine, CA.

34. J. J. P. Stewart, MOPAC 2007, version 7, 290 W Stewart Computational Chemistry, Colorado Springs, CO, 2007.
35. M. J. S. Dewar, E. G. Zoebisch, E. F. Healy, *J. Am. Chem. Soc.*, 1985, **107**, 3902-3909.
36. F. Jensen. Introduction to computational chemistry. Second Edition. John Wiley & Son Ltd, 2007.
37. A. R. Katritsky, V. S. Lobanov, and M. Karelson, (1996). *CODESSA: Reference Manual; Version 2*, University of Florida.